Proceedings of ISFOG 2025
5TH INTERNATIONAL SYMPOSIUM ON
FRONTIERS IN OFFSHORE GEOTECHNICS
Nantes, France | June 9-13 2025

ISBN 978-2-85782-758-0

Micromechanical study of the uplift resistance of offshore rock berm protected pipelines

M. O. Ciantia, M. Previtali, M. J. Brown
School of Science and Engineering, University of Dundee, Dundee, UK

A.J Maconochie
TechnipFMC, Aberdeen, UK

mociantia@dundee.ac.uk; matteo.ciantia@unimib.it

ABSTRACT: Offshore rock dumping in water depths up to 200m to create rockberms is routinely used in both the oil and gas and wind power sectors to provide protection and stability to products laid directly on the seabed, e.g. pipelines, umbilicals and cables. There are significant benefits to be gained from optimising the rockdump volumes used for these purposes including cost reduction, a reduction in the environmental impact on the seafloor and use of primary quarried materials. A key parameter in the design of the rockberms, particularly where they are being used to restrain the product on the seabed from buckling, is the uplift resistance provided by the rockdump. This paper considers the application of the discrete element method (DEM) to model the granular nature of rockdump materials and explores pipeline rock berm interaction to predict the uplift resistance. The non-spherical particle shapes used in the study are obtained through image analysis and laser scanning. The contact model is calibrated using, tilt table and interface testing and validated using angle of repose tests. A 3D DEM plane strain model is developed and the advantages/disadvantages in terms of model construction times and impact on the quality of the results are discussed. The predicted uplift resistance is then compared to physical model tests from the literature and analytical design methods.

Keywords: DEM; Rockfill; Offshore Pipeline protection; Uplift resistance; Rockberms

1 INTRODUCTION

Upheaval buckling is the main failure mode for buried pipelines therefore the main parameter of interest is the vertical uplift resistance, typically assessed using simplified analytical solutions and limit-state analysis.

Historically, experimental (White et al., 2008; Giampa et al., 2017) and numerical (Li et al., 2024) studies have been carried out to improve understanding of peak uplift resistance of pipes buried in sand or clay. An alternative more economically viable protection measure than conventional trench and burial techniques is rock dumping over a surface laid product (Maconochie 2023). Commonly used in water depths up to 200m, angular rock units are dumped in water to create rockberms covering and stabilising pipelines and cables laid directly on the seabed. Because of the deposition method and the angularity of the particles, the rockberm in its final configuration may be very loose but its final state is challenging to characterise insitu. Considering also that shearing behaviour of such angular and large particles has received less attention due to the complexities related with laboratory element testing of large samples, it is not clear if existing analytical predictive method tools that use critical state soil mechanics parameters such as peak friction ϕ^p and dilation ψ angles, perform well in the prediction of uplift resistance for large units such as rock dump.

The Discrete Element Method (DEM) is a numerical tool that in the last decade has proved its ability to replicate granular behaviour in such a realistic way that can be reliably used as a digital twin (Ali et al. 2024; Sharif et al. 2021). With the advancement of computational power, the modelling of realistic particle shape has largely improved and researchers have used DEM to model ballast (Chen et al. 2023) and angular gravels (Ciantia et al 2022) effectively.

This paper presents some results of a DEM numerical study of uplift resistance of offshore rock berm protected pipelines. The numerical results are then compared with available experimental data (Maconochie 2023) and existing analytical methods to gauge their predictive performance.

2 UPLIFT PREDICTION METHODS

For cohesionless soils, such as rock berm material, it is common practice to use a vertical slip surface model, where the uplift resistance generated by a block of material above the pipe is considered. The uplift resistance R is the sum of the weight W of the block and the vertical component of the resistance on the shearing plane (S). The three models typically used are those by Schaminée (1990) (also used in CIRIA C683, *The Rock Manual* (2007)), White et al. (2008), and Giampa et al. (2017).

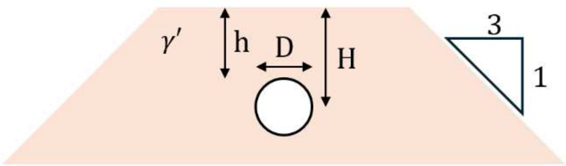

Figure 1: Schematic of the geometry of a rockberm.

Schaminée (1990) defines pullout resistance R as a function of weight of a column of overlying material:

$$R = \gamma' D h + f_d \gamma' h^2 \qquad (1)$$

where γ' is the effective (buoyant) unit weight of the material while D and $h = H - D/2$ are defined as in Figure 1. f_d is an empirical coefficient (assumed ≈0.6 for gravel and rockfill). White et al. (2008) and Giampa et al. (2017) assume a wedge of soil uplifted with shear planes inclined to the vertical at the dilation angle. Under this assumption, the weight per unit depth of the affected soil wedge is:

$$W = \gamma' D H + \gamma' H^2 \tan\psi - \pi\gamma' D^2/8 \qquad (2)$$

where ψ is the dilation angle. To calculate S, White et al (2008) assume a normal effective stress acting on the sliding planes equal to the in-situ value inferred from k_0 conditions. In this case

$$S = \gamma' H^2 (\tan\phi^p - \tan\psi)\left(\frac{(1+k_0)-(1-k_0)\cos 2\psi}{2}\right) \qquad (3)$$

Giampa et al. (2017) reviewed this work and proposed a modified expression for S:

$$S = \gamma' H^2 (\tan\phi^p - \tan\psi)\cos(\phi - \psi) \qquad (4)$$

3 DIGITAL TWIN OF A ROCK BERM

3.1 Angular particle modelling

To model the rock particles rock fragments were individually digitised in 3D using a hand-held Lidar type scanner. Particle size distribution (PSD) and standard particle shape descriptors were digitally determined. Particle sphericity (Sp) is defined as the ratio of the diameters (d_{eq}) of a circle of equivalent area (A_{eq}) to the one circumscribing the particle (d_{cc}). Roundness (R_d) is calculated as the average diameter (d) of circles $_i$ that approximate the curvature of the non-linear portions of contour, normalised by d_{eq} (Mo et al., 2020). Solidity (S) is the ratio of the area of a particle to that of its convex hull (A_{ch}). The same is done with spheres and volumes in 3D. Figure 2 shows the resulting particle size and shape metrics distributions. A 3D sample is produced replicating the scanned volumes at different scales to reproduce the target PSD using polyhedra within the commercial code PFC3D. The software uses the Gilbert-Johnson-Keerthi algorithm to detect contacts between convex bodies, and the Expanding Polytope Algorithm to determine overlaps. Additional details are available in the Itasca PFC3D manual (Itasca, 2025).

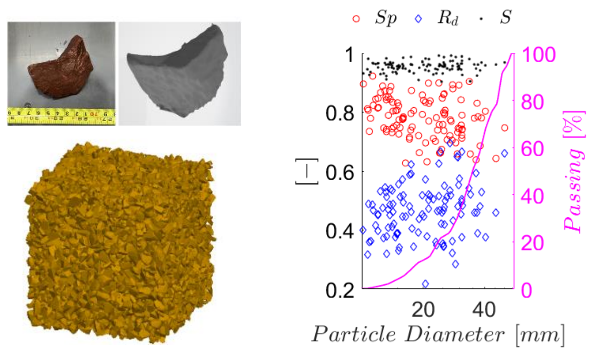

Figure 2: Picture of a real and LIDAR scanned particle, shape parameter distribution against PSD and 3D DEM digital twin for Triaxial compression tests

3.2 DEM contact model parameters

The interparticle behaviour between the polyhedral is modelled using a linear contact model. Following Ciantia et al (2015) a contact shear (k_s) to normal (k_n) stiffness ratio of 0.25 was used and by setting k_n=6 GN/m an effective contact stiffness of 30 MPa was attained. Interface friction angles of particle-particle and particle-pipe contacts were determined through experimental tilt table tests, yielding values of 24 and 27 degrees respectively. To model submerged conditions a reduced gravity of 6.05 m/s^2 was used while particle density ρ_r was set to 2650 kg/m^3.

3.3 Element testing

Following the approach of Ciantia et al (2019) a series of triaxial compression tests on cubic loose and dense samples at variable continent pressures were carried out to obtain the macroscopic shearing behaviour. Samples consisting of ~ 4000 particles were generated within a periodic domain at a confining pressure of 500 Pa. During sample generation interparticle friction was modified to attain loose or dense samples. Once target porosity was attained the calibrated friction coefficient was then reassigned to all particles.

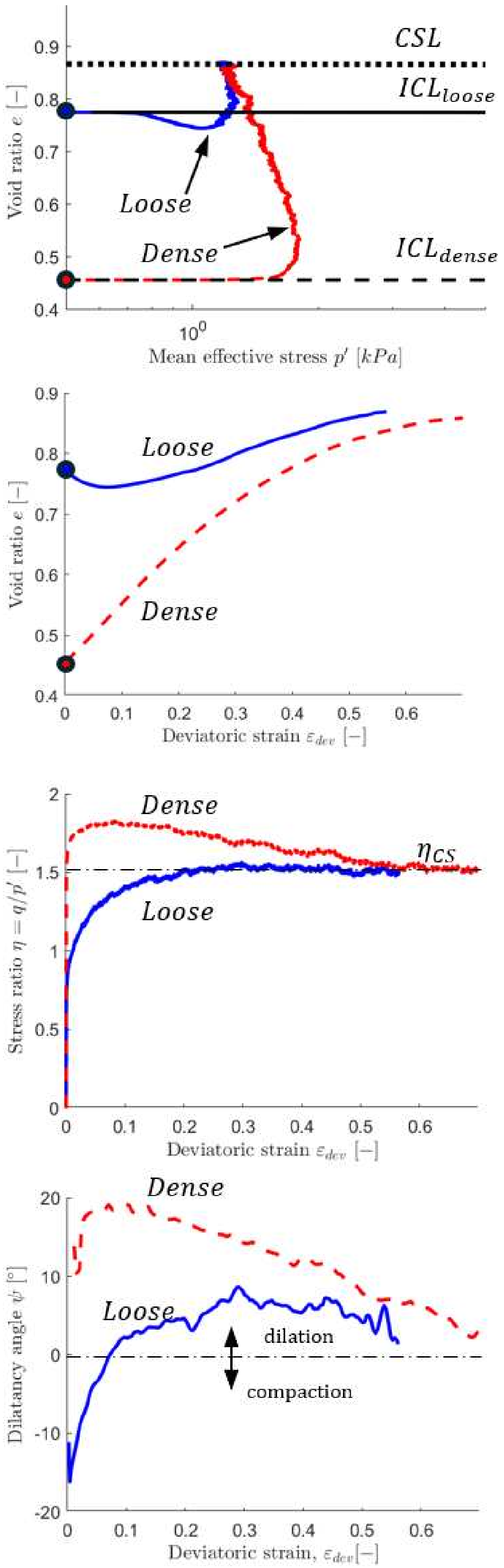

Figure 3: Numerical triaxial response: from top to bottom, compression plane stress paths and void ratio, η=q/p and dilatancy evolution with deviatoric strain.

Samples at different pressures were obtained by progressively increasing the confinement up to 20 kPa to replicate the low levels in a rock berm. While maximum void ratio (e_{max}) is difficult to attain numerically as numerical vibrations of the servo control densify the loose state, the minimum void ratio (e_{min}) is easier to obtain. The values obtained here were deemed acceptable as close to the experimental values from the literature (Abbireddy et al. 2010). Table 1 summarises the mechanical parameters obtained using loose and dense digital samples of the rockdump material. Figure 3 shows the evolution of the stress ratio $\eta = q/p$ and sample void ratio e with deviatoric strains. The dilatancy angle ψ was calculated according to Vermeer & de Borst (1984). As shown by the results, the dense sample is close to the minimum void ratio while the loose one shows some compaction followed by a dilative behaviour indicating a denser than critical state (CS). Nonetheless dilation here is quite limited and peak friction angles correspond to the critical state ones ($\phi^p \sim \phi$).

Table 1: Material parameters from triaxial tests

Parameter		Value	
ψ^p_{loose}	Peak dilatancy loose sample	5.7	[°]
ψ^p_{dense}	Peak dilatancy dense sample	18.6	[°]
ϕ	Critical state friction angle	37.2	[°]
ϕ^p_{dense}	Peak friction angle (dense)	42.8	[°]
ϕ^p_{loose}	Peak friction angle (loose)	37.2	[°]
e_{dense}	Void ratio dense sample	0.43	[−]
e_{loose}	Void ratio loose sample	0.75	[−]
e_{cs}	Void ratio at CS (0.5<p'<100 kPa)	0.85	[−]

3.4 Rock berm model

Plane-strain conditions were obtained in 3D through periodic boundaries in the out-of-plane direction, with a domain thickness of $2.5d_{100}$, (where d_{100} is the maximum particle size dimension) to avoid the same particle being in contact with both boundaries. For spherical particles, this value would correspond to two times the largest diameter. Here, a 2.5 factor is chosen to account for non-spherical shaped grains. The pipe geometry was represented using a non-deformable circular wall. The rock berm geometry was that of an isosceles trapezium, with a flat top 0.5m long and sides inclination of 1/3rd (≈33° see Figure 1). Two different approaches were tested to generate the berm geometry, schematised in Figure 4.

A multi-step pluviation process is used to try and replicate the real process. To this end, the pipe is placed on top of a material sample through a servo-control system, setting the pipe's weight as the target force. The particles are successively pluviated around the pipe. Finally, excess particles are removed at the top of the domain to reproduce the berm geometry at the desired embedment depth H.

The wished-in-place (WIP) approach consists of filling the domain with material at a target porosity and stress state and successively introducing the pipe geometry, removing the DEM particles at its location and cycling the model to stability (i.e. negligible kinetic energy) while servocontrol is used to apply the pipe self-weight. This generation procedure is carried out using the brick replication approach (Ciantia et al. 2018). The relative density for brick replication is obtained by simulating 3D pluviation within a smaller domain.

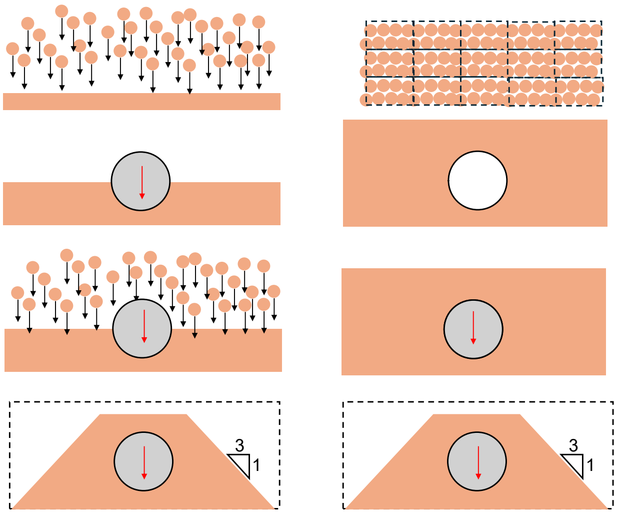

Figure 4: Model generation steps. A) pluviated model setup. b) Wished-in-place setup.

Both models were generated at a mean void ratio of ~ 0.9. After rock berm initialization is completed, the pipe is displaced vertically upwards slowly enough to ensure quasi-static conditions throughout the test. To achieve this, the vertical displacement rate ($\dot{u}$) is such that:

$$\dot{u} < DI/d_{50}\sqrt{\rho_r/p'} \qquad (5)$$

where I (=1E-3) is the system inertia coefficient, d_{50} (=40 mm) is the median particle size and p' is the confining pressure of the material in the region above the pipe. As the two berm generation methods were found to produce very similar resistance curves, considering that the pluviation method takes significantly longer to initialise (weeks compared to hours for WIP), the WIP method was systematically used for model initialization to perform parametric analyses. A pipe, D = 0.315 m covered by four overburden (h) values (0.25, 0.5, 0.75 and 1 m) was tested. This corresponds to H/D values of 1.3, 2.1, 2.9, 3.7. Table 2 summarises the initial conditions for the four simulations performed and Figure 5 shows the cross section of the equilibrated model before imposing the vertical displacement to the pipe. In the following the results of H/D of 2.1 and 3.7 will be presented.

Table 2: Model test initial conditions and runtime

H/D (-)	**H (m)**	**N particles (-)**	p' **(Pa)**	**Simulation times**
1.3	0.25	17110	181	10 days
2.1	0.5	22958	270	9.6 days
2.9	0.75	28851	337	9.2 days
3.7	1	34518	514	9 days

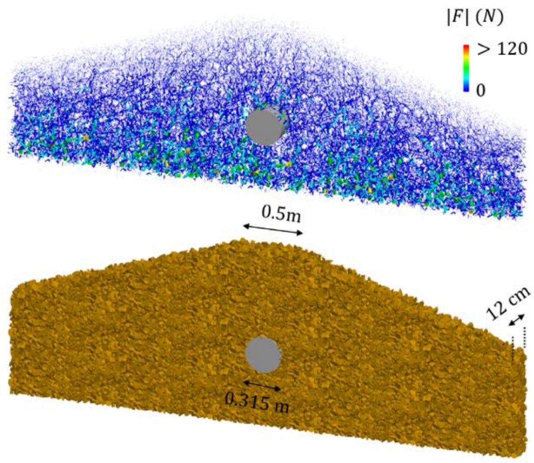

Figure 5: Example of rock berm model in 3D. (a) particle-particle contacts scaled by force, (b) 3D rigidblocks

4 RESULTS AND DISCUSSION

The normalised numerical and experimental force-displacement curves are shown in Figure 6. It is important to note that the experimental results from Maconochie (2023) have been normalised with a dry density ($\gamma_d = 15.2\ kN/m^3$) while the numerical samples had an average initial unit weight of $\gamma' = 8.33\ kN/m^3$. As shown in the figure the H/D=2.1 model trend is very similar to the H/D=2.5 experimental one. Also, the H/D=3.7 simulation is close to the experimental H/D=3.5 result. The DEM results indicate much smaller mobilisation displacements. One possible explanation is that, unlike experiments where system compliance often leads to larger displacements, the DEM results are free from such effects. Considering that this result is obtained by calibrating the DEM model using very simple experiments (see section 3) the results are extremely good and give confidence to the micromechanical approach used.

Given the pullout curves, it is then possible to extract the normalised peak pullout force and compare this with the analytical methods described above (Figure 7). In the figure also the experimental results by Maconochie (2023) are reported. The ψ and ϕ^p values used for the analytical expressions are those corresponding to the loose sample response listed in Table 1.

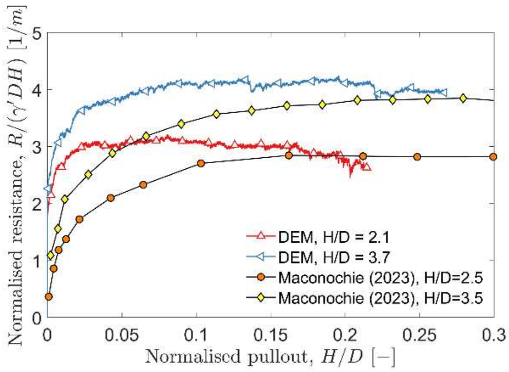

Figure 6:Pullout curves for D = 0.315 m.

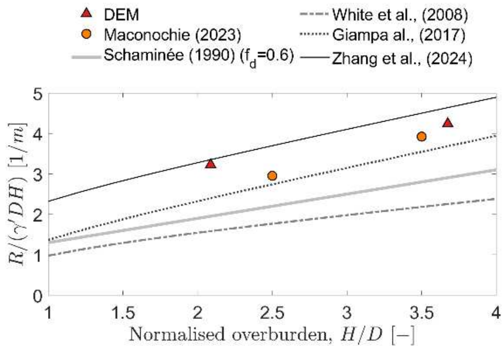

Figure 7: Normalised pullout resistance from DEM simulations, plotted against analytical solutions.

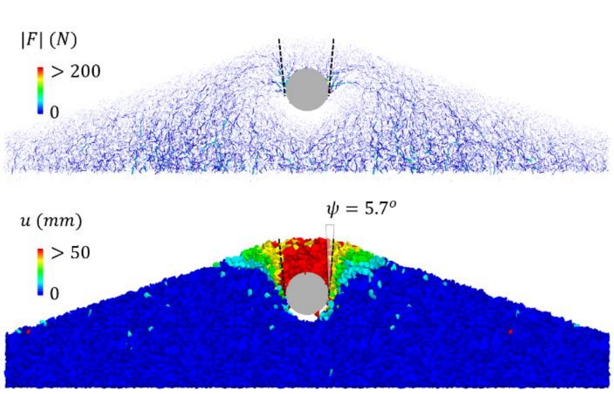

Figure 8: DEM model showing contact forces and particle displacement fields at peak resistance for the H/D=1.3 simulation.

In Figure 7 it is also possible to observe that White et al. (2008) and Schaminée (1990) underestimate both experimental and DEM results. Also, the slope of both models does not seem to capture the results trend. Giampa et al. (2017) on the other hand performs better and can be used to provide a good conservative estimation of pullout strength. This conservative response might be due to an underestimation of the thickness of the shear zone that, as shown in Figure 8, is larger than the dilatancy angle would predict.

Zhang et al., (2024) recently proposed a way to incorporate the weight contribution of this *additional affected zone* induced by enhanced dilation for low confining stress conditions. The additional weight (W_ψ) to add to eq. 2 results in:

$$W_\psi = \gamma'(0.56D + 3.2d_{50})H \tag{6}$$

As shown in Figure 7 the Zhang et al., (2024) approach captures the results for low embedment ratios, while its slightly unconservative for H/D>2.5. The explanation for this is visible in Figure 9 where for low embedment ratios enhanced dilation effects are more pronounced and, in proportion to volume displaced, have a larger influence.

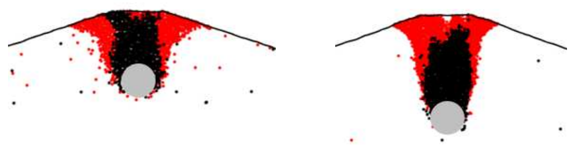

a) b)

Figure 9: Incremental displacement field at peak resistance. H/D: (a) 2.1, (b) 3.7. The red and black areas represent the 90th and 95th percentiles of particle velocities

5 CONCLUSIONS

This paper describes a numerical micromechanical approach to quantify the uplift resistance of pipelines covered by a rock berm. To generate the discrete element model (DEM), a library of real rock berm angular particles obtained using image analysis and lidar scanning, was used. To overcome the limitations of 2D DEM such as porosity measurements, a 3D model was generated under plane-strain conditions by means of out of plane periodic boundaries. It was shown how model generation times can be accelerated by a factor of 10 by employing the Ciantia et al. (2018) brick replication approach. In addition, a set of 3D numerical triaxial test were used to obtain critical state macroscopic values including peak friction ϕ^p and dilation ψ angles, which were required to allow comparison to analytical solutions used by industry.

The model results were compared with experimental data available in the literature and it was found that analytical predictive methods all underpredict the pullout capacity. This is because the models do not properly consider the highly dilatant behaviour of granular material at very low confining stresses. It is also shown that incorporating the additionally affected zone induced by enhanced dilation under low confining pressures improves the predictions at low embedment depths.

Finally, the DEM developed, calibrated using very simple and quick experimental procedures, was shown to be a reliable and successful approach to investigate uplift resistance of offshore rock berm protected pipelines.

AUTHOR CONTRIBUTION STATEMENT

M. O. Ciantia: Conceptualization, Methodology, Software, Writing Original draft. **M. Previtali**: Conceptualization, Formal analysis, Software. **M. J. Brown**: Conceptualization, Writing- Reviewing and Editing. **A. J. Maconochie**: Conceptualization, Writing- Reviewing and Editing

REFERENCES

Abbireddy, C. O. R., & Clayton, C. R. I. (2010). Varying initial void ratios for DEM simulations. *Géotechnique*, 60(6), 497-502.

Ali U., Kikumoto M, Ciantia MO., Cui Y, Previtali M (2024) Why modeling particle shape matters: exploring its impacts on granular behaviour at global and local scales. *ASCE Journal of Geotechnical & Geoenvironmental Engineering*. 150(9)

Chen, J., Vinod, J. S., Indraratna, B., Ngo, T., & Liu, Y. (2023). DEM study on the dynamic responses of a ballasted track under moving loading. *Computers and Geotechnics*, 153, 105105.

Ciantia, M. O., Arroyo, M., Calvetti, F., & Gens, A. (2015). An approach to enhance efficiency of DEM modelling of soils with crushable grains. *Géotechnique*, *65*(2), 91-110.

Ciantia, M. O., Boschi, K., Shire, T., & Emam, S. (2018). Numerical techniques for fast generation of large discrete-element models. *Proceedings of the Institution of Civil Engineers-Engineering and Computational Mechanics*, 171(4), 147-161.

Ciantia, M. O. Arroyo, M., O'Sullivan, C., Gens, A. & Liu, T. (2019) Grading evolution and critical state in a discrete numerical model of Fontainebleau sand, *Géotechnique*. 69(1), 1-15.

Ciantia, M. O., Previtali, M., & Cakir, T. (2022). Experimental and DEM study of monotonic and cyclic simple shear testing of an angular sand. In *Proceedings of the 20th International Conference on Soil Mechanics and Geotechnical Engineering, Sydney 2021* (pp. 661-666). Australian Geomechanics Society.

Garnier, J., Gaudin, C., Springman, S. M., Culligan, P. J., Goodings, D., Konig, D & Thorel, L. (2007). Catalogue of scaling laws and similitude questions in geotechnical centrifuge modelling. *International Journal of Physical Modelling in Geotechnics*, 7(3), 01-23.

Giampa, J. R., Bradshaw, A. S., & Schneider, J. A. (2017). Influence of dilation angle on drained shallow circular anchor uplift capacity. *International Journal of Geomechanics*, 17(2), 04016056.

Itasca (2025). Itasca Software Guide.

Li, X., Kouretzis, G., & Thoeni, K. (2024). Discrete Element Modelling of uplift of rigid pipes deeply buried in dense sand. *Computers and Geotechnics*, 166, 105957

Maconochie A. J. (2023) Up-lift resistance of pipelines within a rock berm. In *Offshore Site Investigation Geotechnics 9th International Conference Proceeding* (pp. 508-1297). Society for Underwater Technology.

Mo, P. Q. (2020). Internal rolling method for particle shape evaluation and reconstruction. *Plos one*, 15(11), e0242162.

Rock Manual, (2007). The Use of Rock in Hydraulic Engineering. CIRIA, second ed. CIRIA, CUR, CETMEF, London. Published by C683, ISBN 978-0-86017-683-1 and 5.

Schaminée, P. E. L., Zorn, N. F., & Schotman, G. J. M. (1990, May). *Soil response for pipeline upheaval buckling analyses: Full-scale laboratory tests and modelling.* In Offshore Technology Conference (pp. OTC-6486). OTC.

Sharif, Y., Brown, M., Ciantia, M., Lutenegger, A., Kumar, P., Patra, S., & Haldar, S. (2021). Using discrete-element method hindcasting of screw pile performance for practical design. *Géotechnique Letters*, 11(4), 1-7.

Vanden Berghe, J. F., Cathie, D., & Ballard, J. C. (2005). *Pipeline uplift mechanisms using finite element analysis.* In Proceedings of the 16th International Conference on Soil Mechanics and Geotechnical Engineering (pp. 1801-1804). IOS Press.

Vermeer, P. A., & De Borst, R. E. N. É. (1984). Non-associated plasticity for soils, concrete and rock. *HERON, 29 (3), 1984*.

White, D.J., Cheuk, C.Y., Bolton, M.D., (2008). The uplift resistance of pipes and plate anchors buried in sand. *Géotechnique* 58, 771–779.

Zhang, X., Knappett, J. A., Ciantia, M. O., Leung, A. K., Wang, H., & Liang, T. (2024). Root size effects on transverse root-soil interactions. *Computers and Geotechnics*, 165, 105860.